

# Chapter 8

## OCULAR EFFECTS OF ULTRAVIOLET LASER RADIATION

JOSEPH A. ZUCLICH, PhD\*

---

### INTRODUCTION

- Military Relevance
- General Background

### ABSORPTION PROPERTIES OF OCULAR TISSUES

### CORNEAL EFFECTS

- Clinical Observations—Photokeratitis
- Action Spectra
- Photoablation
- Pulsewidth Dependence
- Cumulative Effects

### LENS EFFECTS

- Transient Clouding and Cataracts
- Lens Fluorescence

### RETINAL EFFECTS

- Photochemical Effects—Morphology
- Veiling Glare

### SUMMARY

\*Senior Scientist/Consultant, Science Applications International Corporation, 1100 Northwest Loop 410, Suite 700, San Antonio, Texas 78213

## INTRODUCTION

The consequences of exposure to ultraviolet (UV) radiation are known to include acute and chronic effects in the cornea, lens, and retina of the primate eye. The purpose of this chapter is to describe the nature of the various UV laser-induced ocular pathologies and to discuss the operative mechanisms of damage in each case. Understanding of damage mechanisms and delineation of the exposure parameters to which each ocular tissue is the most sensitive have helped guide development of many military and biomedical applications of lasers described in this volume.

### Military Relevance

The development of the laser in the late 1950s to early 1960s coincided historically with early successes in the manned space program, which spurred military and biomedical interest in understanding bioeffects of UV radiation at dose levels encountered in the extraterrestrial environment. The UV laser offered compelling advantages over the use of conventional sources of light such as arc lamps or high-power searchlights. Lasers provided the means to deliver intense, carefully directed exposures to in-vitro and in-vivo targets while allowing accurate diagnostic measurements of exposure parameters. Thus, as UV-emitting lasers first became available in the 1970s, researchers used them to supplement and complement ongoing investigations of biological effects of UV radiation.

As research and development yielded a greater variety of UV lasers, military interest continued to evolve and expand. The US Navy provided early support for the development of UV/short-visible wavelength lasers that might be used in undersea communications. Excimer lasers, now widely used for corrective refractive surgery, have been studied extensively as a means to preserve and enhance the visual performance of pilots, other specialized aircrew, and combat personnel. Low-level, portable UV laser systems are widely used in photo-therapeutic and germicidal applications. Some remote bio-detection systems utilize a tripled neodymium-doped yttrium aluminum garnet (Nd:YAG) laser (355 nm) to identify a variety of specific aerosol agents. Diode lasers

with near-UV/blue wavelength outputs can induce a veiling glare that results from the fluorescence of the ocular lens; this is a possible way to disrupt visual performance without causing permanent ocular injury.

### General Background

Proteins and nucleic acids are the molecular building blocks of living tissue; they are largely transparent to visible and near-infrared wavelengths but can have strong absorption bands in the UV range. At UV wavelengths, photons may be sufficiently energetic to excite electrons of absorbing bio-molecules from the inert ground state to a highly reactive state. Before relaxing back to the ground state, the excited molecules may react with neighboring molecules to form a "photoproduct" that is not innate to the cell. The photoproduct is often disruptive to normal cell functioning and may eventually lead to cell death. The macroscopic observation of an abnormality and any physical sensation or other manifestation of the photodamage may be delayed, typically for several hours beyond the time of the UV exposure. Depending on the location and extent of damage, the resulting pathology may be described as a "lesion," "erythema," "inflammation," or "burn."

In order to understand the nature, extent, and recovery of laser-induced injury to the eye, and to establish protection and guidance for others (eg, military personnel) who may be exposed, careful dose-response data in nonhuman primates described effects of UV radiation on the cornea, lens, and/or retina. In each case, the primary target tissue is determined by the specific combination of exposure parameters (wavelength, peak power, pulsewidth, pulse repetition frequency, and total energy delivered).<sup>1,2</sup> Effects may be acute or chronic, and the implicated mechanism of damage may be photochemical, photoablative, or thermal. The photochemical damage mechanism described above is most specific to UV wavelengths. Photoablative and thermal processes, also prevalent throughout other regions of the wavelength spectrum, are described elsewhere in this volume.

## ABSORPTION PROPERTIES OF OCULAR TISSUES

Figure 8-1 depicts a schematic cross-sectional view of the primate eye, illustrating the passage of a collimated laser beam through the pupil and focused on the retina. The UV absorption properties of the components of the ocular medium (cornea, aqueous, lens,

and vitreous) are illustrated in Figure 8-2 (calculated from the data of Boettner and Dankovic<sup>3</sup>). As can be seen, far-UV wavelengths (200–300 nm) are strongly absorbed by the cornea and do not penetrate deeper into the eye. Near-UV radiation (300–400 nm) is largely

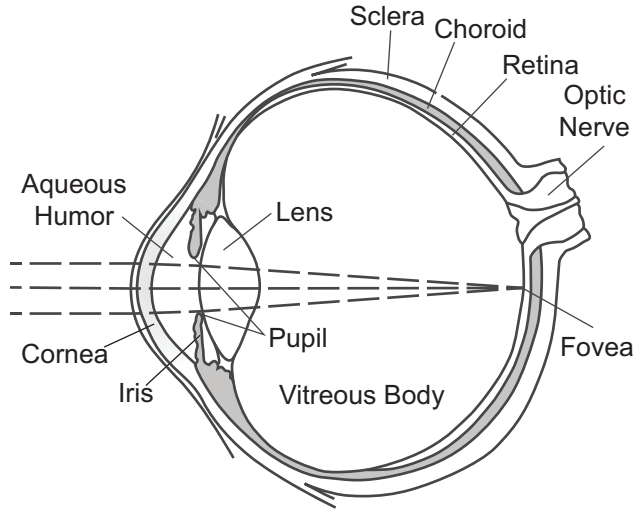


**Figure 8-1.** Schematic cross-sectional view of the primate eye.

transmitted by the cornea but strongly absorbed by the lens, which serves to protect the retina from ambient environmental UV radiation. The aqueous and vitreous humors have absorption spectra that run paral-

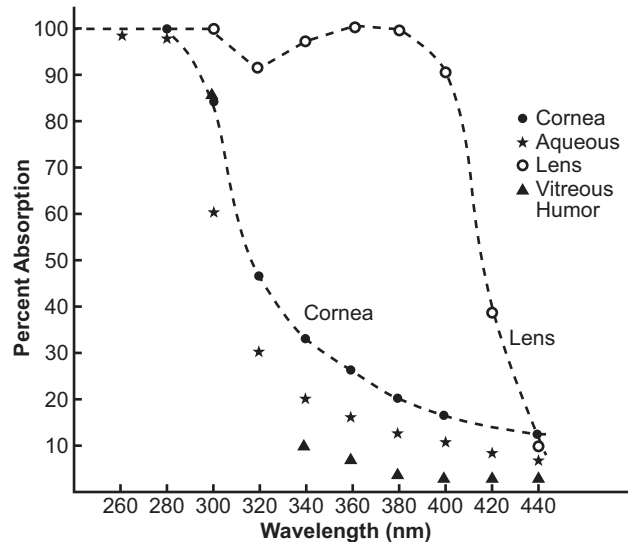


**Figure 8-2.** Ultraviolet absorption spectra of ocular components of the primate eye. The absorption spectra for the rhesus and human eyes are virtually identical. Reproduced with permission from: Zuclich JA. Ultraviolet-induced photochemical damage in ocular tissues. *Health Phys.* 1989;56:671-682.

lel to that of the cornea, but with lower absorption coefficients for UV and visible wavelengths due to relatively lower cellular and higher aqueous contents. The composite transmission spectrum of the primate ocular medium (Figure 8-3) is calculated from the absorption properties of its individual components.<sup>3</sup> Little incident UV radiation is transmitted through the ocular medium to reach the retina. However, at ~320 nm and again at ~400 nm, approximately 1% of the corneal incident radiation does reach the retina and is absorbed by its cellular constituents.

From the ocular component absorption properties as described above, it is anticipated that the cornea will be the primary if not the only target tissue affected by far-UV wavelengths. Within the range of ~320 to ~400 nm, the lens is generally the primary tissue affected by near-UV radiation. Given that the focusing power of the eye more than offsets transmission losses through the ocular medium, the small percentage of UV radiation that reaches the retina at ~320 and ~400 nm could also have consequences for retinal tissue. The remaining sections of this chapter will consider, in turn, the corneal, lenticular, and retinal effects observed following exposure to UV laser radiation.

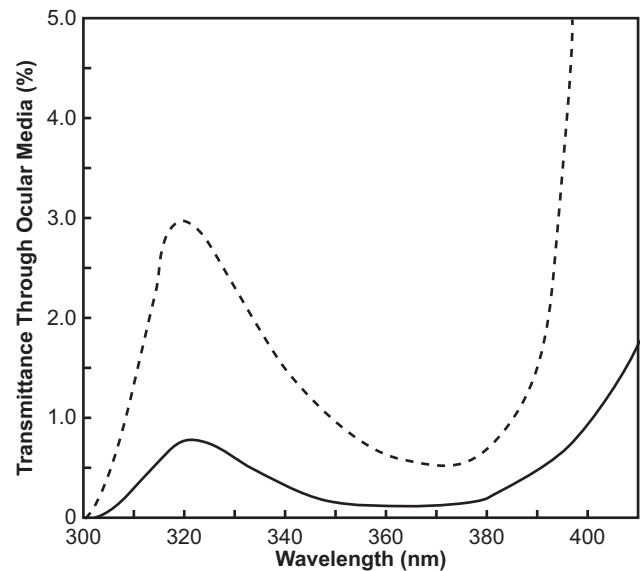


**Figure 8-3.** Transmission spectrum of rhesus ocular medium for near-ultraviolet radiation. The solid line represents direct transmission. The dashed line represents total (direct plus forward scattered) transmission. Reproduced with permission from: Zuclich JA. Ultraviolet-induced photochemical damage in ocular tissues. *Health Phys.* 1989;56:671-682.

## CORNEAL EFFECTS

### Clinical Observations—Photokeratitis

Figure 8-4 illustrates a clinical manifestation of UV-induced photochemical damage to the cornea of a rhesus monkey.<sup>4</sup> The clouding observed on the right side of the cornea developed over a period of 24 hours following UV irradiation of a circular area 2 mm in diameter. The UV source was a krypton-ion laser emitting at ~350 nm. At this wavelength, the radiant exposure required to induce an observable clouding was ~60 J/cm<sup>2</sup>. Although this effect is wavelength dependent, it is not related to the coherent properties of the laser radiation. The same irradiance threshold can be obtained using a conventional source (eg, mercury arc lamp) filtered to yield a comparable wavelength.

Clinical reports of photokeratitis (snow blindness, exposure to welder's arc, etc) indicate that suprathreshold whole-eye UV exposure may produce considerable discomfort and possibly severe pain, which begins several hours after exposure and persists for

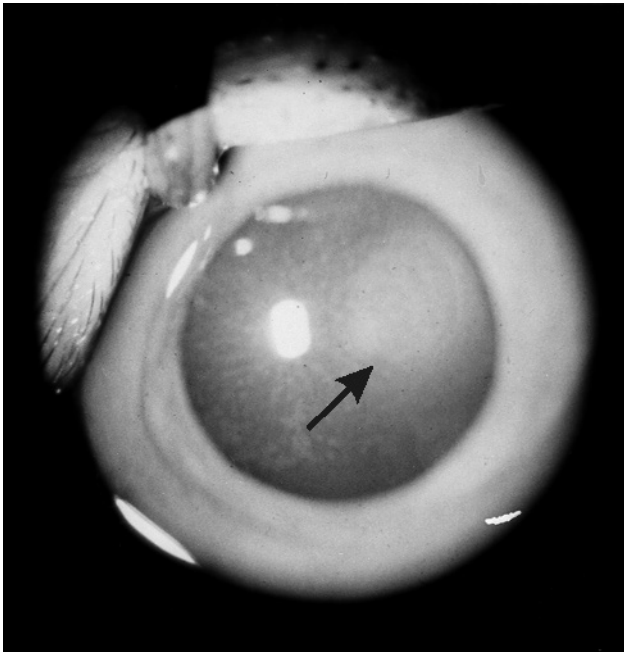


**Figure 8-4.** Corneal clouding (arrow) induced in a rhesus monkey following ultraviolet irradiation of a 2-mm diameter area of cornea by ultraviolet output of krypton-ion laser (350.7 and 356.4 nm). The bright reflection seen to the left of the lesion is due to the photographic flash. Reproduced with permission from: Zuclich JA. Ultraviolet-induced photochemical damage in ocular tissues. *Health Phys.* 1989;56:671–682.

24 hours or more.<sup>5</sup> In addition to the clouding shown in Figure 8-4, symptoms can include conjunctivitis, tearing, photophobia, and the sensation of sand or other granules in the eye. Generally, all symptoms resolve within 48 hours. For the threshold determination experiments referenced above,<sup>4</sup> UV exposures were limited to small areas covering the center of each cornea; following exposure, the behavior of the animal subjects was asymptomatic of eye irritation.

Figures 8-5 and 8-6 are photomicrographs showing the cellular effects associated with the macroscopic UV-induced corneal clouding seen in Figure 8-4.<sup>6</sup> In Figure 8-5, the left edge of the photo shows normal tissue characterized by a regular array of basal cells and fairly even staining of the epithelial cells. The right half of the photo shows the edge of a corneal lesion, with the irradiated tissue exhibiting a significant thinning of the epithelium relative to the non-irradiated tissue. Thinning of the epithelium occurs as damaged surface epithelial cells break up and are sloughed into the tear layer. The premature breakup and sloughing of epithelial cell debris into the tear layer lead to the delayed physical discomfort experienced following a suprathreshold UV exposure. At the same time, the UV exposure causes an initial depression of cell division in the basal layer.<sup>7,8</sup> Following a quiescent period generally lasting no more than 24 hours, there is increased mitotic activity until the epithelial cell population grows back to its normal level.

Figure 8-6 illustrates the central region of the lesion shown in Figure 8-5. Here, the basal cells of the epithelium are swollen and irregularly shaped. Heavy staining indicates radiation damage in the vast majority of the cells. In a subsequent experiment (not shown), the corneal tissue of a rhesus monkey subjected to an identical exposure was fixed at 48 hours (rather than at 18 h postexposure as shown in Figures 8-5 and 8-6). The resulting tissue in that case was essentially normal save for the thickness of the epithelial layer, which had not yet fully recovered.

### Action Spectra

The action spectrum (threshold vs wavelength) for near-UV-induced corneal damage in the rhesus eye is plotted in Figure 8-7.<sup>9</sup> The action spectrum was determined by using an arc-lamp source filtered to bandwidths of 10 nm. Thresholds varied significantly over the near-UV wavelengths, ranging from ~10 J/cm<sup>2</sup> at 320 nm to over 300 J/cm<sup>2</sup> at 400 nm. When corrected for variation in corneal absorption,<sup>3</sup> the curve has a shape similar to that found for near-UV inactivation of bacteria.<sup>10</sup>

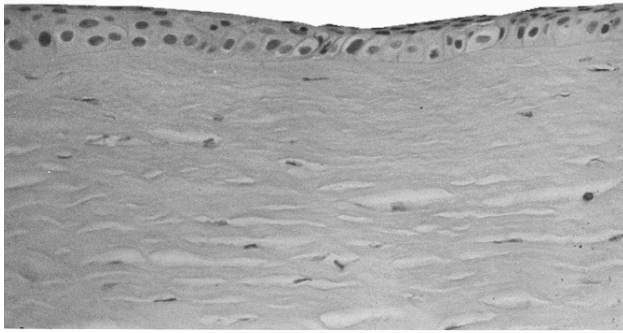


**Figure 8-5.** Photomicrograph of rhesus corneal tissue from an eye exposed to ultraviolet output of krypton-ion laser (350.7 and 356.4 nm). The tissue was fixed in glutaraldehyde in cacodylate buffer and stained with hematoxylin and eosin. This photo shows normal tissue (left) and the edge of a corneal lesion with irradiated tissue on the right. Reproduced with permission from: Zuclich JA. Ultraviolet-induced photochemical damage in ocular tissues. *Health Phys.* 1989;56:671–682.

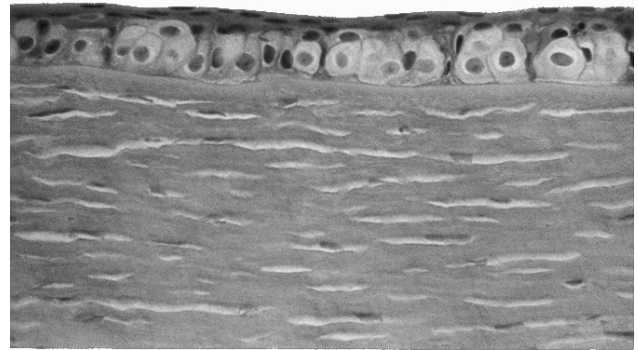


**Figure 8-6.** Center of the corneal lesion shown in Figure 8-5. Reproduced with permission from: Zuclich JA. Ultraviolet-induced photochemical damage in ocular tissues. *Health Phys.* 1989;56:671–682.

The action spectrum for far-UV corneal damage is plotted in Figure 8-8. This plot is based on data from Pitts and colleagues, who showed closely similar curves for rabbit, monkey, and human subjects.<sup>5,11</sup> The cornea exhibits maximum sensitivity to far-UV exposure at ~260 to 280 nm, where the threshold is ~5 mJ/cm<sup>2</sup>. This wavelength region coincides with the first absorption bands of the aromatic amino acids of proteins and of the common bases of nucleic acids.<sup>12</sup>

**Photoablation**

Also plotted in Figure 8-8 are the corneal damage thresholds for ~20-ns pulses from XeCl, krypton fluoride (KrF), and argon fluoride (ArF) excimer lasers, at wavelengths of 308, 248, and 193 nm, respectively.<sup>13–15</sup> The XeCl and KrF excimer thresholds are in reasonable agreement with the action spectrum obtained using low-power conventional sources with exposure times in the order of seconds. However, the ArF threshold is 2 to 3 orders of magnitude below what would be anticipated by extrapolation of the action spectrum to 193 nm. This reflects the greater efficiency of a photoablative damage mechanism for the short-pulse, high-peak power excimer laser exposures relative to that of a photochemical mechanism, which dominates with long, low-power exposures.

Photoablation may be the most efficient tissue damage mechanism when exposure conditions create a photon flux that is large enough to overwhelm molecular bonding and thus produce an explosive dispersion

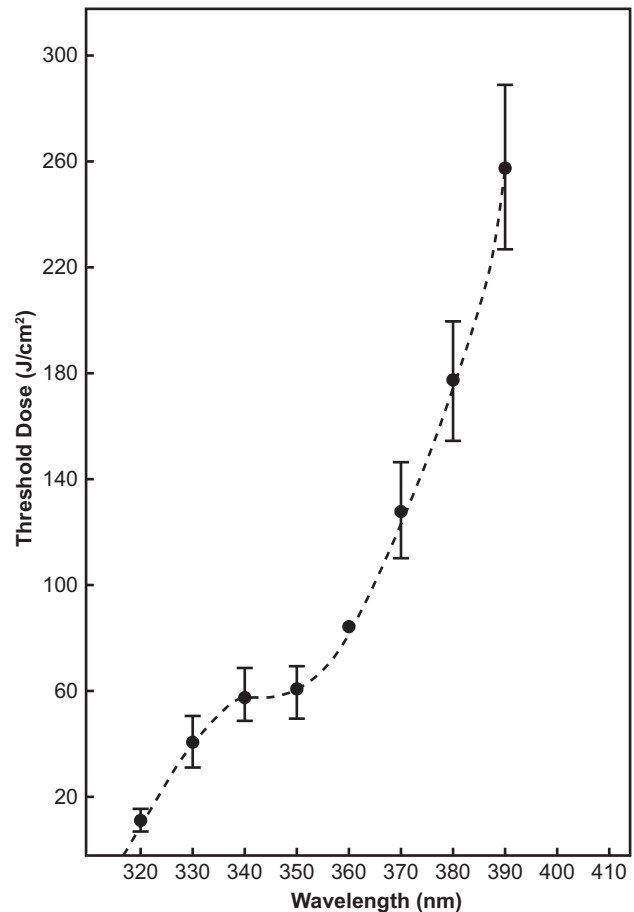


**Figure 8-7.** Action spectrum for near-ultraviolet-induced corneal damage in the rhesus monkey.

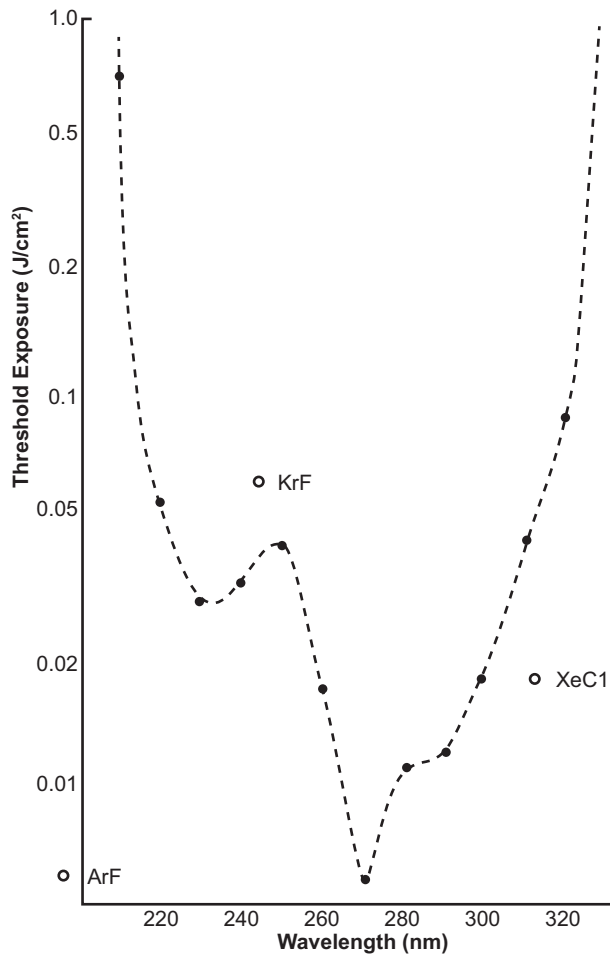


**Figure 8-8.** Action spectrum for far-ultraviolet-induced corneal damage in the rabbit. Open circles are excimer laser thresholds. Reproduced with permission from: Zuclich JA. Ultraviolet-induced photochemical damage in ocular tissues. *Health Phys.* 1989;56:671–682.

of small fragments from the irradiated surface. If the laser radiation is also strongly absorbed by the irradiated tissue, little if any light penetrates beyond the small volume of ablated tissue. Hence, surrounding tissue will remain undamaged. However, a high absorption coefficient is not a requirement for an ablative surface process. Short-pulsewidth infrared and visible-wavelength lasers have also been used successfully to ablate ocular tissues via a plasma-mediated process that results from optical breakdown at the irradiated focal plane.<sup>16</sup> A typical ablation rate observed in corneal tissue is 1- $\mu\text{m}$  depth of tissue ablated per 1  $\text{J}/\text{cm}^2$  of excimer laser radiation incident at the surface. By repetitive laser pulsing, a very precise and controlled tissue cutting process is achieved. Additional discussion of the photoablative process may be found in the

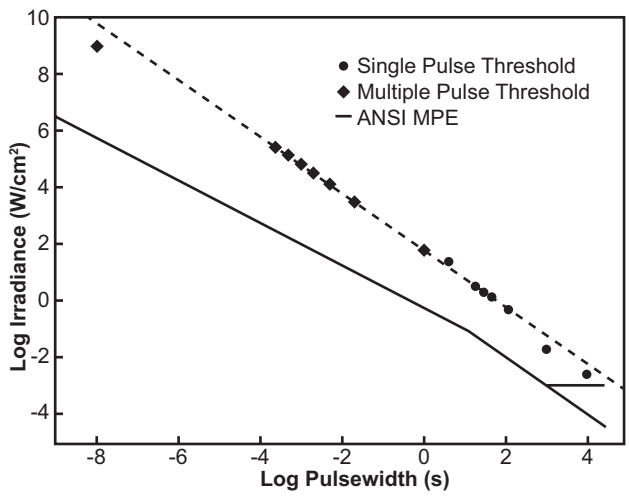


**Figure 8-9.** Log-log plot of corneal threshold as a function of pulsewidth. The dashed line represents a best fit to the experimental data. The solid line is the American National Standards Institute (ANSI) laser safety standard maximum permissible exposure (MPE) for near-ultraviolet laser radiation (315–400 nm). The horizontal solid-line segment represents the ANSI MPE for exposures  $>10^3$  s, as it existed before the 1986 revision of the standard. Reproduced with permission from: Zuclich JA. Ultraviolet-induced photochemical damage in ocular tissues. *Health Phys.* 1989;56:671–682.

work of Srinivasan and Trokel.<sup>17–19</sup> A photomicrograph of a corneal cut observed after repetitive pulsing with ArF excimer laser radiation is pictured in a 1990 article by Zuclich.<sup>20</sup>

**Pulsewidth Dependence**

Commercially available UV sources cover very broad ranges of exposure parameters. These range from low-power continuous wave (CW) sources to short-pulsewidth lasers (nanosecond or less) with very high peak powers (megawatt or greater). Figure 8-9 demonstrates the variation in corneal threshold across 12 orders of magnitude of pulsewidth.<sup>2</sup> These data represent corneal lesions induced by krypton-ion and argon-ion laser radiation (350–360 nm), except for the point at 10 ns, which resulted from nitrogen laser radiation at 337 nm. The dashed line is an equal energy curve equivalent to a corneal radiant exposure of 60  $\text{J}/\text{cm}^2$ . All of the thresholds, including those for single-pulse and multiple-pulse exposures, fall quite close to the equal energy line. Therefore, a reciprocity relationship exists between irradiance and pulsewidth. This provides quantitative evidence that a single-photon photochemical mechanism is operative over

the entire range of pulsewidths examined at near-UV wavelengths. Functionally, this suggests that a UV hazard assessment can be determined in terms of radiant exposure (ie, total number of photons absorbed by the exposed tissue), and that within certain limits (discussed below), the threshold is dependent upon neither the rate at which the energy is delivered nor whether the UV dose is delivered by a single exposure or any sequence of repeated exposures.

For UV wavelengths other than ~350 nm, the corneal threshold at any given pulsewidth would be higher or lower than that shown in Figure 8-9, in accordance with the wavelength dependence depicted by the action spectra (Figures 8-7 and 8-8). The solid line shown in Figure 8-9 is the American National Standards Institute (ANSI) maximum permissible exposure (MPE) for near-UV (315–400 nm) laser radiation.<sup>21</sup> This standard runs roughly parallel to the experimental data, allowing a margin of safety of a factor of 10 or more.

### Cumulative Effects

Another aspect of UV-induced corneal damage that has been examined quantitatively is the cumulative effect of multiple pulses or repeated long exposures.<sup>22</sup> Multiple-pulse threshold data (see Figure 8-9) show that exposures have a net additive effect indicative of the total energy delivered. However, at some point, this additive effect levels off, which indicates that the cornea has a repair or recovery mechanism, or that it can replace damaged epithelial cells with a fresh supply of normal cells.

To quantify the cumulative effect for long or repeated exposures, corneal thresholds were determined for two identical exposures to ~350-nm radiation while time between the two exposures was varied.<sup>22</sup> Figure 8-10 shows the results of one such series of experiments. The point on the ordinate is the single-pulse corneal threshold for exposure to UV krypton-ion laser radiation. The remaining points are cumulative thresholds, that is, total energy doses from two identical subthreshold (if taken independently) exposures. The result is a monotonically increasing trend of cumulative threshold dose with time between exposures. The cumulative threshold approaches twice the single-pulse threshold for longer time intervals. This value would be the upper limit for the threshold if repair was completed between exposures. However, the thresholds for intervals of 5, 7, and 10 days between exposures fall ~10% short of twice the single-pulse threshold. This could indicate a small residual effect due to less-than-complete repair (during the time between

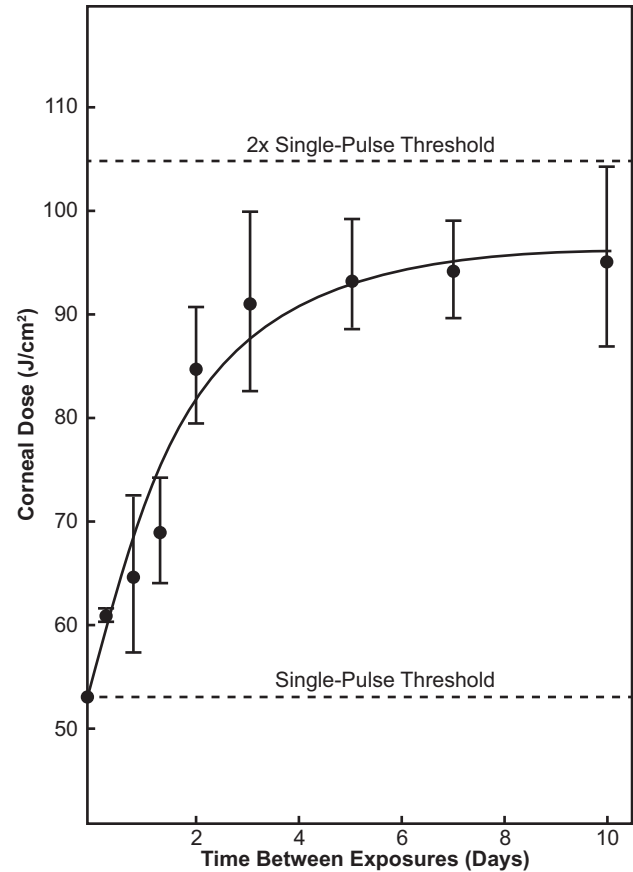


**Figure 8-10.** Repair of corneal epithelial tissue following sub-threshold exposures to near-ultraviolet (UV) laser radiation. The UV source was a krypton-ion laser (350.7 and 356.4 nm). The data points are corneal thresholds for rhesus monkeys subjected to two identical exposures separated by the indicated intervals. The solid line is a least squares fit to the data. Reproduced with permission from: Zuclich JA. Ultraviolet-induced photochemical damage in ocular tissues. *Health Phys.* 1989;56:671–682.

exposures) or to enhanced corneal sensitivity related to the administration of drugs, radiation, or both during the initial exposures.

The solid line in Figure 8-10 represents a best fit to the data assuming that the trend of the corneal threshold ( $Th$ ) is governed by an exponential repair process:

$$Th = c_1 + c_2(1 - e^{-kt})$$

where  $k$  is the repair rate constant,  $c_1$  and  $c_2$  are fitting constants,  $e$  is the base of the natural logarithms (approximately 2.71828), and  $t$  is time. The rate of repair ( $k^{-1}$ ) found from a nonlinear regression calculation (yielding a least squares fit to the data) is equal to ~46 hours.<sup>22</sup> Knowing the rate constant,  $k$ , one can calculate the effective dose of any sequence of repeated

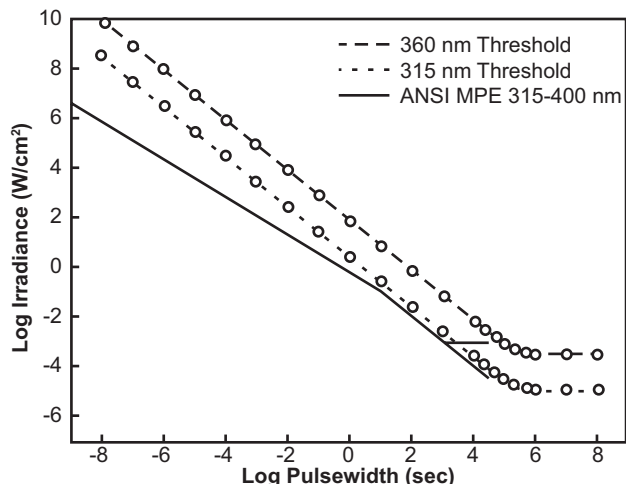


**Figure 8-11.** Log-log plot of corneal threshold as a function of pulsewidth according to the exponential repair model. Curves are shown for 360 nm (dashed line) and 315 nm (dotted line) for comparison to the American National Standards Institute (ANSI) maximum permissible exposure (MPE) (solid line), which applies to the wavelength band from 315 nm to 400 nm. The horizontal solid line segment represents the ANSI MPE for exposures  $>10^3$  s as it existed before being revised to reflect the quantitative repair rate determinations. Reproduced with permission from: Zuclich JA. Ultraviolet-induced photochemical damage in ocular tissues. *Health Phys.* 1989;56:671–682.

exposures. This is important in any situation in which personnel would be exposed to UV radiation on successive days. With such a slow repair rate (46 hours), cumulative effects would occur from one day to the next.

Figure 8-11 shows the behavior of the corneal threshold versus pulsewidth curve according to the exponential repair model. The curve levels off for exposure times greater than  $10^5$  seconds ( $>24$  hours). Roughly speaking, there is a total additive effect of all exposures that occur within a given 24-hour interval.

**TABLE 8-1**

**THRESHOLDS FOR TRANSIENT LENS OPACITIES IN THE RABBIT**

Wavelength (nm)	Corneal Threshold (J/cm <sup>2</sup> )	Lens Threshold (J/cm <sup>2</sup> )
290	0.012	>3.0
295	0.02	0.75
300	0.052	0.15
305	0.07	0.30
310	0.055	0.75
315	2.25	4.5
320	7.25	12.6
325	18.0	>50

Data source: Pitts DG. A comparative study of the effects of ultraviolet radiation on the eye. *Am J Optom Physiol Optics.* 1978;50:19–35.

This additive effect tapers off for exposures separated in time by more than 24 hours. Recognizing the cumulative effect described above, the ANSI laser safety standard for near-UV radiation (315–400 nm) defines an MPE (solid line of Figure 8-11) that follows an equal energy dose for exposure durations from 10 seconds to  $3 \times 10^4$  seconds (~8 hours).

The proposed exponential repair model and the behavior of the threshold versus pulsewidth curve in Figure 8-11 are specific to the corneal epithelium. Different results may be found for other tissues that have different repair capacities or more complex (multiparametric) repair processes. However, Griess and Blakenstein examined the additive effect and repair following low-level (nonthermal), blue-light retinal exposures and have concluded that a simple exponential repair model applies in that case as well.<sup>23</sup> The rate of repair found for retinal tissue was ~96 hours compared to 46 hours for the corneal epithelium.

**LENS EFFECTS**

**Transient Clouding and Cataracts**

As was seen in Figure 8-2, most of the incident near-UV radiation is transmitted through the cornea and absorbed by the lens. Due to the “yellow pigment” found in primate lenses,<sup>24</sup> the lens has an absorption peak centered at 365 nm. Much evidence relates chronic or age-related cataract to long-term (lifetime) exposure to ambient UV, but discussion of this extensive body of epidemiological, biochemical, and histological evidence on chronic cataract is beyond the scope of this

chapter. For more information on chronic cataract, see Waxler and Hitchens.<sup>25</sup>

Acute cataract induced via photochemical processes can occur following exposure to a narrow band of wavelengths from 290 to 325 nm. Table 8-1 compares the corneal and transient lens opacity thresholds for wavelengths in this range.<sup>26</sup> Depending on exposure dose, the lens clouding may be transient or permanent. Permanent opacities (cataracts) are observed following exposure to doses that are a factor of two or more above the transient lens opacity thresholds.<sup>26</sup> There-

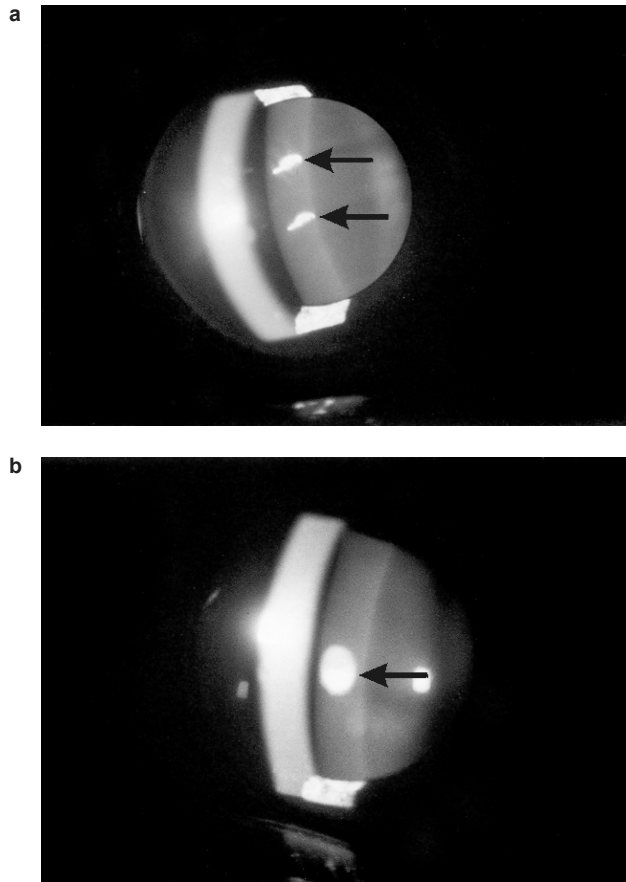


**Figure 8-12.** Cataracts (arrows) induced in rhesus monkey lens as a result of thermal insult from ultraviolet laser radiation. The cataracts are located at the anterior surface of the lens. Reflections can also be seen from the corneal surface, the posterior surface of the lens, and the lids (above and below). (a) Two cataracts induced by 10-ns pulses from nitrogen laser (337 nm). (b) Cataract induced by continuous wave radiation from argon-ion laser (351.1 and 363.8 nm).  
Reproduced with permission from: Zuclich JA. Ultraviolet-induced photochemical damage in ocular tissues. *Health Phys.* 1989;56:671–682.

fore, the lens effect can represent a more serious injury than the corneal damage (which generally is repaired within 48 hours). For wavelengths shorter than ~295 nm, corneal absorption is sufficient to protect the lens. At wavelengths greater than ~325 nm, acute cataract induction via photochemical processes is not observed.

There is, however, another type of lens hazard associated with lasers and other intense sources of wavelengths near the lens absorption band centered at 365 nm. At high irradiance levels, immediate thermal damage to the lens is possible because the incident energy is deposited primarily near the anterior surface of the lens. Examples of such acute cataracts are

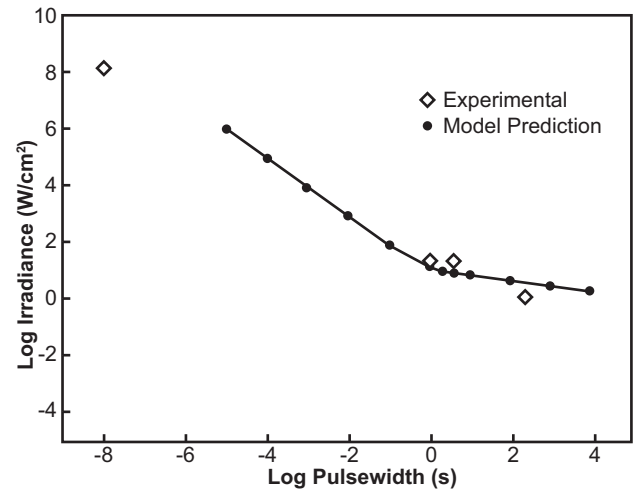


**Figure 8-13.** Log-log plot of lens threshold as a function of pulsewidth. The solid line is the predicted thermal threshold for primate lens damage induced by 350-nm radiation. Reproduced with permission from: Zuclich JA. Ultraviolet-induced photochemical damage in ocular tissues. *Health Phys.* 1989;56:671–682.

shown in Figure 8-12. The two bright opacities seen in Figure 8-12 (a) were induced in a rhesus lens by trains of 10-ns pulses from a nitrogen laser emitting at 337 nm.<sup>4</sup> The peak power of the 10-ns pulses was ~1 MW. The elongated shape of the lesions reflects the shape of the nitrogen laser beam. Figure 8-12 (b) shows an opacity induced by a CW argon-ion laser. In this case, the laser power was ~1 W at 351.1 nm and 363.8 nm (emitted simultaneously) with a beam diameter of ~2 mm. An exposure time of 1 second was sufficient to result in cataract formation.

This type of immediate lens opacity appears to be adequately described by a thermal damage mechanism.<sup>4</sup> On a plot of irradiance versus pulsewidth such as that seen in Figure 8-13, lens threshold data, although sparse, follow the solid line, which represents the damage threshold predicted by thermal model calculations. This trend contrasts with that of the corneal thresholds data, which follow the equal energy curve for exposure durations up to 10<sup>5</sup> seconds. The corneal and lenticular threshold versus pulsewidth curves are overlaid in Figure 8-14 to demonstrate that for long exposures, the corneal photochemical damage can be induced at much lower irradiance levels. For shorter exposures (1 s or less), there may be a greater hazard to the lens. However, it is important to note that there is no simple demarcation of lens and corneal susceptibility based on exposure duration. Corneal and lens thresholds exhibit different wavelength dependencies, reflecting the damage mechanisms operative in each case.

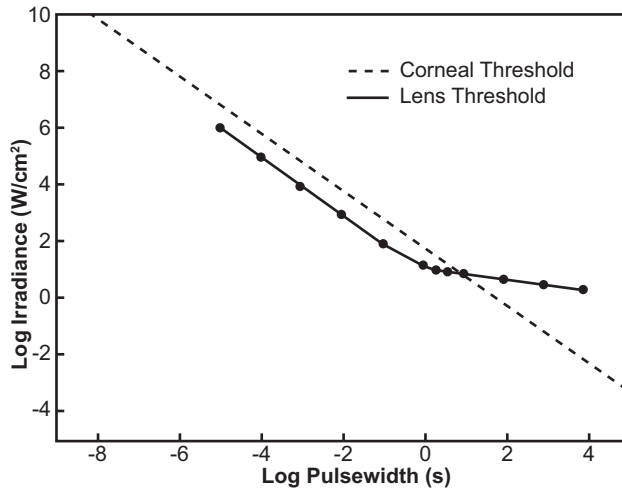


**Figure 8-14.** Overlay of lens thermal threshold versus pulsewidth curve of Figure 8-13 (solid line) and corneal photochemical threshold versus pulsewidth curve of Figure 8-9 (dashed line).  
 Reproduced with permission from: Zuclich JA. Ultraviolet-induced photochemical damage in ocular tissues. *Health Phys.* 1989;56:671–682.

**Lens Fluorescence**

The development of “blue” diode lasers (here referring to diodes emitting at near-UV through short-visible wavelengths) and their potential widespread use in consumer electronics raised the prospect of escalating rates of ocular exposures and possible claims of eye injury or visual problems, even at non-injurious exposure levels. A similar scenario unfolded following the widespread dissemination of small, inexpensive (virtually throw-away) red diode lasers.<sup>27–30</sup> In the case of “blue” diode lasers, however, there is an interesting variation with respect to the nature of potential visual disruption. Because the majority of incident radiation throughout the near-UV to blue wavelength range is absorbed by the lens, visual consequences arise not only from the small percentage of incident radiation that is transmitted directly to the retina (see Figure 8-3), but also (and primarily) from the blue-green lens fluorescence emission induced by this wavelength range. The fluorescing lens can be an intraocular source of veiling glare that is dispersed across the entire visual field. This effect may be intense enough to impair visual function.

Figure 8-15 illustrates the fluorescence spectrum recorded from an excised nonhuman primate lens upon excitation with 360 nm radiation (~10-nm bandwidth) from an arc-lamp source.<sup>31</sup> The trailing edge of the excitation envelope is seen at the left edge. When

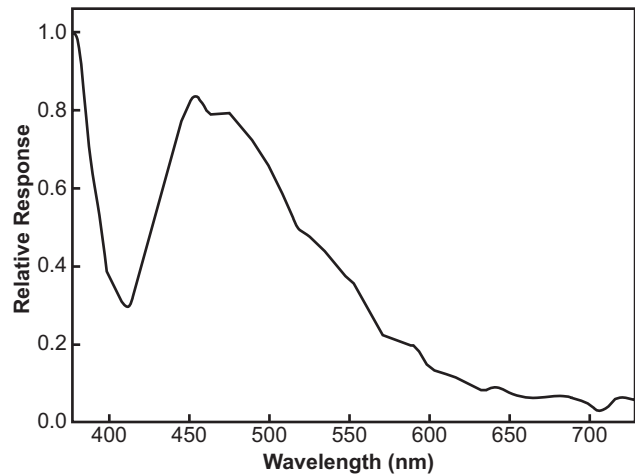


**Figure 8-15.** Fluorescence of excised rhesus lens excited by 360-nm radiation from an arc-lamp source. Reproduced with permission from: Zuclich JA, Glickman RD, Menendez AR. In situ measurements of lens fluorescence and its interference with visual function. *Invest Ophthalmol Vis Sci.* 1992;33:410–415.

the excitation wavelength was varied across the range from 350 to 430 nm, the fluorescence spectrum retained the same general appearance, but its peak shifted to slightly longer wavelengths.<sup>31–33</sup> Table 8-2 summarizes the results of spectroradiometer/photometer measurements of the fluorescence intensity as the exciting

**TABLE 8-2**  
**FLUORESCENCE INTENSITIES MEASURED FROM EXCISED RHESUS LENSES**

Excitation Parameters		Emission Measurements	
Wavelength (nm)	Irradiance (mW/cm <sup>2</sup> )	Radiance (W/sr/m <sup>2</sup> )	Luminance (cd/m <sup>2</sup> )
350	0.019	4.5 × 10 <sup>-4</sup>	0.034
360	0.092	9.6 × 10 <sup>-4</sup>	0.16
400	0.054	5.3 × 10 <sup>-4</sup>	0.13
430	0.064	6.2 × 10 <sup>-4</sup>	0.18

cd: candela  
 sr: steradian  
 Reproduced with permission from: Zuclich JA, Glickman RD, Menendez AR. In situ measurements of lens fluorescence and its interference with visual function. *Invest Ophthalmol Vis Sci.* 1992;33:410–415. Copyright: Association for Research in Vision and Ophthalmology.

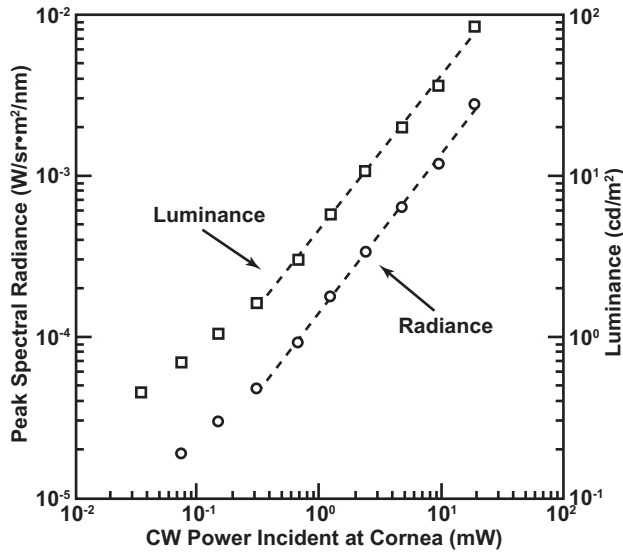


**Figure 8-16.** Peak spectral radiance (circles, left ordinate) and luminance (squares, right ordinate) of lens fluorescence as a function of continuous wave laser power. The slopes of regression lines fit to the radiance and luminance data both approximate 1.0 (actual: radiance = 0.984,  $r = 0.999$ ; luminance = 0.956,  $r = 0.999$ ).

CW: continuous wave

r: regression

sr: steradian

Reproduced with permission from: Zuclich JA, Glickman RD, Menendez AR. In situ measurements of lens fluorescence and its interference with visual function. *Invest Ophthalmol Vis Sci.* 1992;33:410–415. Copyright: Association for Research in Vision and Ophthalmology.

wavelength varied from 350 nm to 430 nm. It is readily seen that after equating for source irradiance, both fluorescence radiance and luminance remained relatively constant over this wavelength range. However, as the exciting wavelength was increased above 430 nm, fluorescence intensity dropped rapidly due to the increasing transmission of the lens.

An in-vivo experiment was conducted to support the hypothesis that fluorescence veiling glare could reach visually debilitating levels in a living subject (anesthetized rhesus monkey).<sup>31</sup> A 413-nm krypton-ion laser was used as the exciting source, and a telephotometer was used to measure the lens fluorescence intensity as a function of excitation intensity. Figure 8-16 shows peak spectral radiance and photopic luminance, each plotted as a function of CW laser power. Both curves exhibit a slope of 1.0 (dashed lines) with no sign of saturation of the emitted fluorescence below the maximum exposure level of 18 mW. Higher exciting intensities were not used with the live subjects due to the risk of inducing

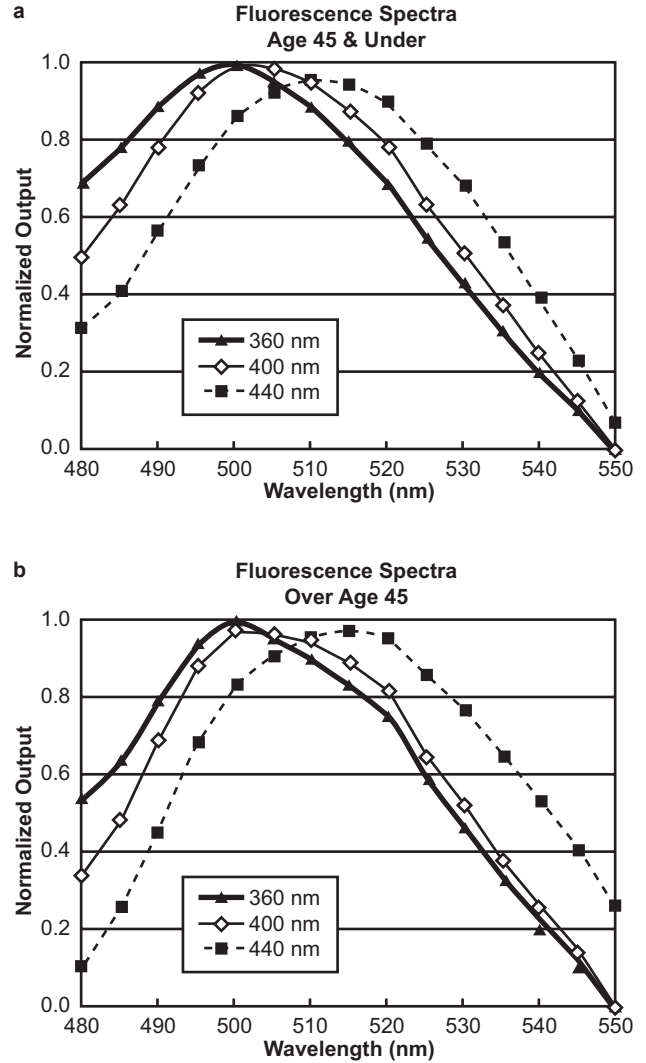


**Figure 8-17.** Fluorescence spectra induced in younger (a) or older (b) lenses by three exciting wavelengths.

thermal damage to the retina or lens. However, with excised lenses, the CW-laser intensity was taken as high as 100 mW. This yielded a fluorescence luminance of ~2,000 cd/m<sup>2</sup>, again without saturation of the fluorescent chromophore.

These findings were later extended to the human.<sup>34</sup> Fluorescence properties measured from human lenses (provided by participating eye banks) were qualitatively and quantitatively similar to those previously reported for nonhuman primates.<sup>31</sup> Typical fluorescence spectra induced by 360-, 400-, and 430-nm arc-lamp excitation are shown in Figure 8-17. Again, excitation wavelengths longer than the ~365-nm lens absorption peak resulted in a more red-shifted fluorescence. However, induced fluorescence had approximately the same luminous and radiant intensities for any

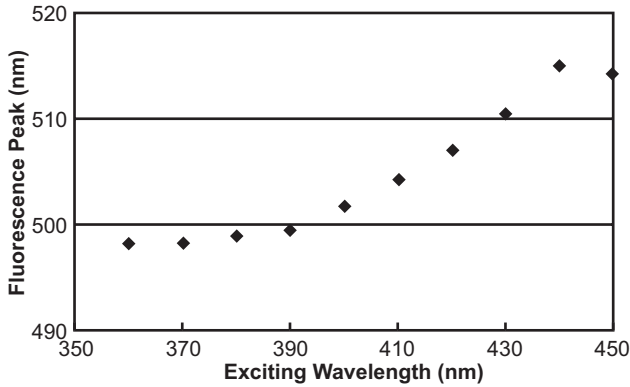


**Figure 8-18.** Variation of fluorescence peak wavelength as a function of exciting wavelength (averaged over all lenses).

exciting wavelength within the range of 350 to 430 nm. Figure 8-18 shows a plot of the peak wavelength of the fluorescence spectrum as a function of exciting wavelength. The only apparent deviation from a monotonically increasing function occurs for 450-nm excitation, where the fluorescence intensity was weak and assignment of a peak wavelength for the broad spectral output was problematic.

Numerous investigators have examined the age dependence of absorption and scattering in the human lens and the consequent age dependence of the near-UV induced lens fluorescence. The age variation in transmission of the human lens is illustrated in Figure 8-19 by a spectral plot of the fraction of the incident radiation transmitted directly through the lens for three age categories.<sup>34</sup> These measurements were obtained with the radiometer detector head placed first at the

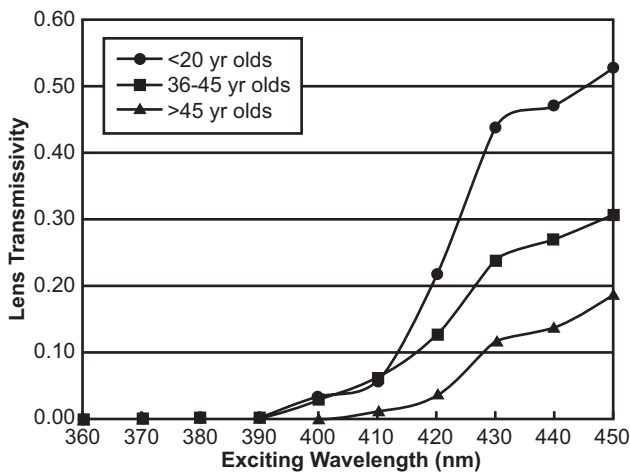


**Figure 8-19.** Human lens transmission spectra for three age categories.

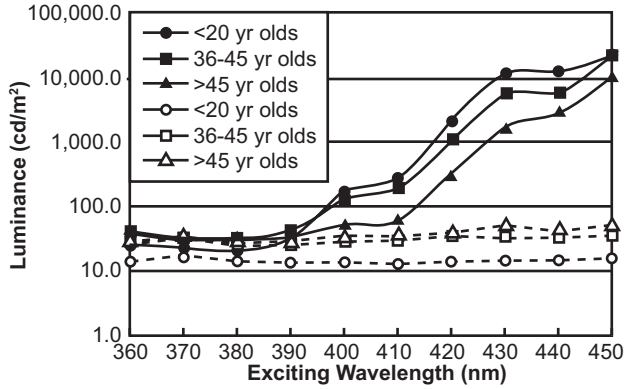


**Figure 8-20.** On-axis (solid lines) and 40° off-axis (dashed lines) fluorescence luminance measurements plotted as a function of exciting wavelength for each age category (normalized to 1-mW incident laser power).

position where the lens would be mounted and then directly behind the mounted lens. Thus, Figure 8-19 illustrates on-axis transmission/absorption spectra of human lenses. It shows that the young lenses had measurable transmission above ~390 nm and exhibited a rapidly increasing transmission for excitation  $\geq 410$  nm, whereas the older lenses were virtually opaque to wavelengths  $\leq 405$  nm and only rose to ~20% direct transmission at 450 nm.

Figure 8-20 shows the analogous (on-axis) plots of lens fluorescence luminance for the same three age categories. With excitation wavelengths  $\geq 390$  nm,

**TABLE 8-3**

**COMPARISON OF LUMINOUS INTENSITIES FROM NONHUMAN PRIMATE LENSES AND HUMAN EYE BANK LENSES**

Exciting Wavelength (nm)	Normalized Luminance Rhesus Lenses*	Normalized Luminance Eye Bank Lenses <sup>†</sup> (cd/m <sup>2</sup> ÷ W/cm <sup>2</sup> )
350	1.80	9.96
360	1.74	9.85
400	2.40	11.1
430	2.80	15.2

\*From Table 8-2; luminance divided by irradiance of exciting source.

<sup>†</sup>Averaged across all lenses (all age categories).

Data source: Zuclich JA, Previc FH, Novar BJ, Edsall PE. Near-UV/blue light-induced fluorescence in the human lens: potential interference with visual function. *J Biomed Optics*. 2005;10:44021-1-7.

measured luminous intensity increased rapidly with increasing wavelength. This is due primarily to the increasing direct transmission of the source. For shorter exciting wavelengths, where the contributions of the directly transmitted radiation are minimal, all age categories showed approximately the same fluorescence luminous intensity.

Figure 8-20 also depicts off-axis luminance of the three age categories as measured at 40° from the axis of irradiation. In contrast to the on-axis measurements, the off-axis results show little dependence upon excitation wavelength. The luminance data were also strikingly similar to the nonhuman primate results reported in Table 8-2. This can be seen in Table 8-3, where the

luminance values from Table 8-2 are normalized versus the respective source irradiances to yield a relatively constant ratio (central column of Table 8-3). Analogous results from the eye-bank lenses (averaged across all age categories) show virtually the same trend (right-hand column of Table 8-3). It is noted that normalized lens luminance is ~5 times higher in the human lens than in the nonhuman primate lens; however, this is not considered a sufficient basis to conclude that either fluorescence efficiency or visual disruption is greater in the human. (Experimental approaches used for human and nonhuman subjects were not entirely analogous; different detecting instruments, aperture sizes, and detector head placements were used).

## RETINAL EFFECTS

### Photochemical Effects—Morphology

The hazard to the retina from laser radiation or from any other effectively collimated source is that the focusing power of the eye can result in a much higher power density at the back of the eye than was incident at the cornea. For UV wavelengths, this retinal hazard is mitigated but not necessarily eliminated by strong absorption by the ocular medium.

The lens is the primary ocular filter of near-UV radiation, and it effectively cuts off transmission to

the retina at the short wavelength end of the visible spectrum. However, an important feature of the lens absorption spectrum (see Figure 8-2) is the small window centered at ~320 nm. At this wavelength, the cornea is not strongly absorbing. Thus, a small amount of UV (~1% of a direct transmission) can reach the retina (see Figure 8-3). It has been shown that the retina is considerably more sensitive to wavelengths near this narrow transmission window than to longer UV wavelengths, which overlap the lens absorption band centered at ~365 nm.<sup>35</sup> This potential retinal hazard was

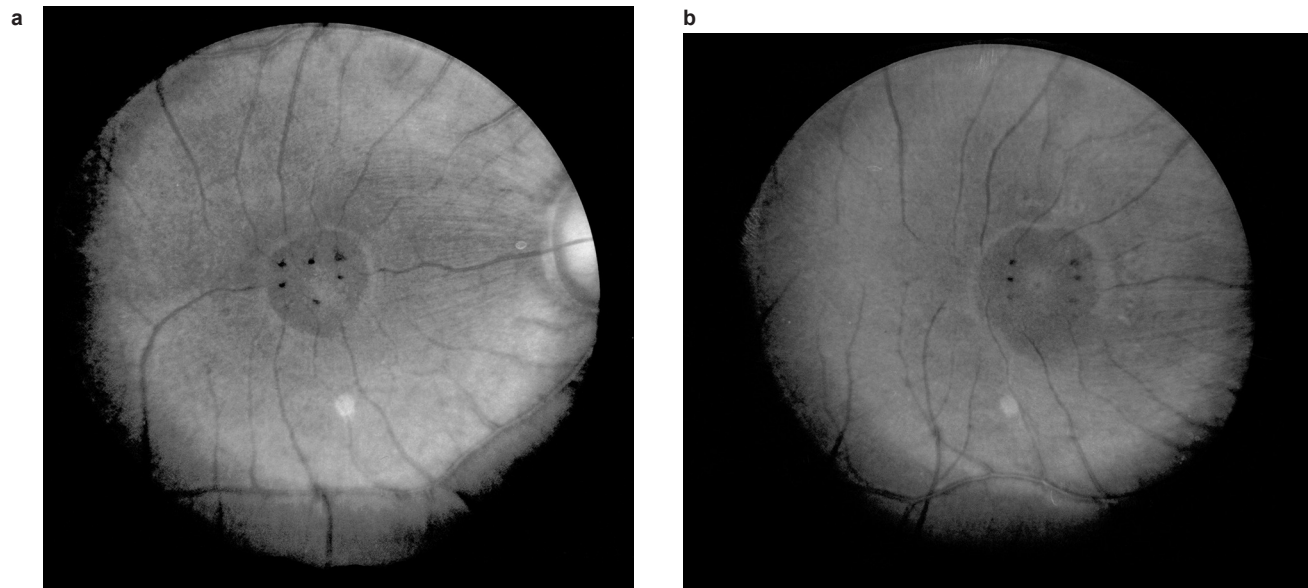


**Figure 8-21.** Retinal lesions induced in maculae of rhesus eyes exposed to the 325-nm output of a helium-cadmium laser. (a) Three-by-three array of macular lesions induced with a constant laser power (20 mW) but varying exposure times. (b) Two-by-four array of macular lesions induced with varying laser powers ( $\leq 20$  mW).

Reproduced with permission from: Zuclich JA. Ultraviolet-induced photochemical damage in ocular tissues. *Health Phys.* 1989;56:671-682.

TABLE 8-4

COMPARISON OF OCULAR THRESHOLDS FROM HELIUM-CADMIUM AND KRYPTON-ION LASERS

Laser Source	Corneal Threshold		Retinal Threshold	
	Radiant Exposure (J/cm <sup>2</sup> )	Energy Dose (J)	Radiant Exposure (J/cm <sup>2</sup> )*	Energy Dose (J)*
Helium-cadmium-UV (325 nm) < 1% transmitted to retina	14	0.28	3.61 × 10 <sup>-1</sup>	7.6 × 10 <sup>-3†</sup>
Krypton-UV (350.7 and 356.4 nm) < 1% transmitted to retina	67	0.89	> 670	> 8.9
Krypton-blue (476 nm) ~60% transmitted to retina	—	—	4.4 × 10 <sup>-2</sup>	2.5 × 10 <sup>-3†</sup>

\*incident at cornea

†comparable pulsewidths (350 ms)

—: no data

Reproduced with permission from: Zuclich JA. Ultraviolet-induced photochemical damage in ocular tissues. *Health Phys.* 1989;56:671–682.

identified with a helium-cadmium (He-Cd) laser that emits at 325 nm. At exposure levels well below the corneal threshold for 325 nm (14 J/cm<sup>2</sup>), darkly pigmented spots developed (over a period of several hours) on the exposed retina of a rhesus monkey (Figure 8-21).<sup>35</sup> Lesion diameters were typically 50 to 100 μm. The time frame of development closely resembled that for the slowly developing corneal clouding described previously and is also comparable to the development of skin erythema induced by UV radiation. Retinal lesions maintained their darkly pigmented appearance for at least several months (as long as the exposed subjects were monitored).

The lesions shown in Figure 8-21 were induced during experiments in which both laser power and exposure time were varied. It was found that there was a total energy requirement (and not a peak power threshold) necessary to induce the darkly pigmented retinal lesions.<sup>35</sup> This evidence suggests a photochemical mechanism of damage.

Table 8-4 compares the retinal threshold for 325-nm radiation (0.36 J/cm<sup>2</sup>) to the corneal threshold for the same wavelength and to the corresponding thresholds for two other wavelengths. The efficiency of the 325-nm UV photons is striking compared to the other cases. In the 350- to 360-nm region, near the lens absorption peak, argon-ion or krypton-ion laser radiation induced no observable retinal effect even with exposures well in excess of corresponding corneal thresholds. Compared with the blue laser emission (> 60% of the incident radiation transmitted to the retina), the 325-nm photons (~1% transmission) are more effective in inducing retinal damage.

Retinal sensitivity to UV wavelengths is further demonstrated by the data of Ham et al,<sup>36</sup> who measured retinal thresholds in the aphakic rhesus eye for a number of visible and UV wavelengths. Their results are summarized in Table 8-5, where the numbers shown in the right-hand column demonstrate the relative retinal sensitivity without the filtering effect of the ocular lens. The shorter the wavelength, the more efficient the retinal photochemical damage

TABLE 8-5

RETINAL THRESHOLDS FOR ULTRAVIOLET EXPOSURES IN THE APHAKIC RHESUS

Wavelength (nm)	Energy at Cornea (J)*	Calculated Retinal Irradiance (W/cm <sup>2</sup> )
488 <sup>†</sup>	—	0.77
405	0.41	0.15
380	0.24	0.081
350	0.20	0.054
325	0.23	0.05

\*100-s exposures

†normal (phakic) eye

—: no data

Data sources: (1) Ham WT, Mueller HA, Ruffolo JJ, Guerry D, Guerry RK. Action spectrum for retinal injury from near-ultraviolet radiation in the aphakic monkey. *Am J Ophthalmol.* 1982;93:299–306. (2) Ham WT Jr, Mueller HA, Sliney DH. Retinal sensitivity to damage from short wavelength light. *Nature.* 1976;260:153–155.

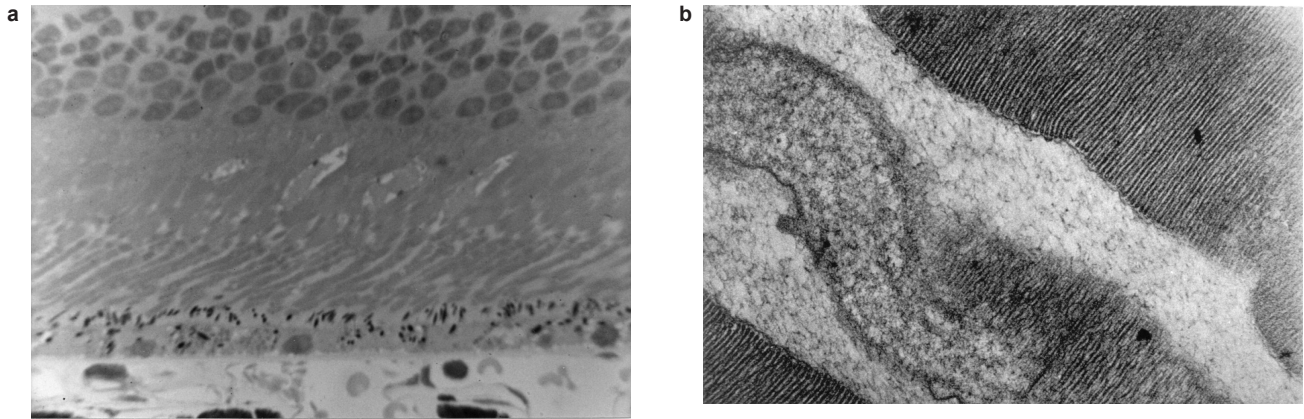


**Figure 8-22.** Morphology of retinal damage induced by the 325-nm output of a helium-cadmium laser. (a) Light micrograph ( $\times 850$ ) of a lesion resulting from a  $0.95 \text{ J/cm}^2$  exposure (incident at cornea). Necrotic inner segments are seen separated by intact cells. (b) Electron micrograph ( $\times 21,000$ ) of tissue subjected to a  $3 \text{ J/cm}^2$  exposure (incident at cornea). A degenerating photoreceptor outer segment is seen adjacent to receptors, which are normal in appearance. Reproduced with permission from: Zuclich JA. Ultraviolet-induced photochemical damage in ocular tissues. *Health Phys.* 1989;56:671–682.

mechanism. Note that the 325-nm wavelength is probably close to the shortest wavelength for observation of any retinal effect. At shorter wavelengths, the absorption of the ocular media begins to overwhelm all other factors.

The morphology of UV laser-induced retinal lesions in the phakic eye is illustrated in Figure 8-22.<sup>37</sup> Figure 8-22 (a) is a light micrograph of a section of rhesus retina that was exposed to a suprathreshold dose of 325-nm laser radiation 24 hours before fixing the tissue. Exposure durations were on the order of 1 second, and exposures were confined to the macula. Several instances of necrosis of photoreceptor inner segments are observable, as well as loss of adjacent nuclei in the outer nuclear layer. Figure 8-22 (b) is an electron micrograph of similarly exposed tissue, showing a degenerating photoreceptor outer segment adjacent to apparently normal cone segments on either side. These histologic studies thus identify the photoreceptors as the primary site of retinal damage. The retinal pigment epithelium (RPE) and other retinal layers appear normal. By contrast, Ham et al<sup>36</sup> observed significant damage to the RPE as well as to photoreceptors in the aphakic rhesus retina exposed to near-UV radiation for 100-second and 1,000-second periods.

Retinal radiant exposures calculated using best estimates of retinal image size and transmission of the ocular medium at 325 nm are comparable for the threshold in the phakic eye (see Table 8-4) and that reported by Ham et al in the aphakic eye (see Table 8-5). However, it should be noted that the exposure times differed by  $\sim 3$  orders of magnitude; this factor may account for differences noted in the pathology.

Although the implications for visual function are not fully understood, it is important to stress that the near-UV exposures did induce photoreceptor damage and that the funduscopically observed retinal lesions (darkly pigmented spots) were permanent in nature.

### Veiling Glare

As noted previously, near-UV to blue wavelengths (360–430 nm) can induce a blue-green fluorescence in the primate lens. The measured luminance of that fluorescence can be sufficient to interfere with visual function. Lens fluorescence is dispersed over the entire visual field, imposing a “veiling glare” that reduces the contrast of the perceived view. A unique experiment used visual evoked potentials (VEPs) to provide an objective measure of the visual deficit associated with the fluorescent glare induced in live subjects by low-level laser radiation.<sup>31</sup> The VEPs were recorded from anesthetized rhesus monkeys with scalp electrodes placed over the foveal projection area of the visual cortex. The anesthetized subject (with a dilated pupil) viewed a stimulus monitor projected to the eye from a pellicle beam-splitter set in front of a fundus camera. The center of the projected stimulus field was aligned along the optic axis of the fundus camera. The subject’s fundus was viewed on a television monitor using only the infrared component of the fundus camera’s viewing light. This was done to avoid disrupting the dark-adaptation state. During the VEP recording session, 413-nm krypton-ion laser radiation was introduced by directing the collimated

beam through the pupil at an angle of  $45^\circ$  to the optic axis of the fundus camera (and the subject's visual axis). The small percentage of laser radiation transmitted through the ocular medium<sup>38</sup> was incident on the peripheral retina at a spot well off the field of view of the fundus video monitor. Laser power incident at the cornea was 0.5 to 1.5 mW in a 5-mm diameter beam.

Laser exposure conditions for the VEP experiment were chosen to approximate the safety standard MPE levels for exposure to a visible wavelength laser<sup>21,39</sup> while minimizing the possibility of a direct glare effect. The exposure wavelength had a low luminous efficiency (0.002) and the collimated beam was directed  $45^\circ$  off axis, where the predicted glare effect is negligible.<sup>40</sup>

Figure 8-23 depicts VEP amplitude plotted as a function of stimulus contrast with and without CW-laser radiation. In the absence of lens fluorescence effects, the two response curves should coincide. Instead, in the presence of the laser radiation, the VEP amplitudes were reduced for all values of stimulus grating contrast. Similar results were generated in each of three VEP recording sessions with two rhesus subjects. Observed reductions in VEP amplitude were attributed to the fluorescence glare.

Data from excised human lenses provide an objective distinction between contributions to the veiling glare that arise from direct transmission of the exciting source radiation versus those attributable solely to the induced lens fluorescence. Zuclich et al<sup>34</sup> performed luminance measurements and generated CIE (Inter-

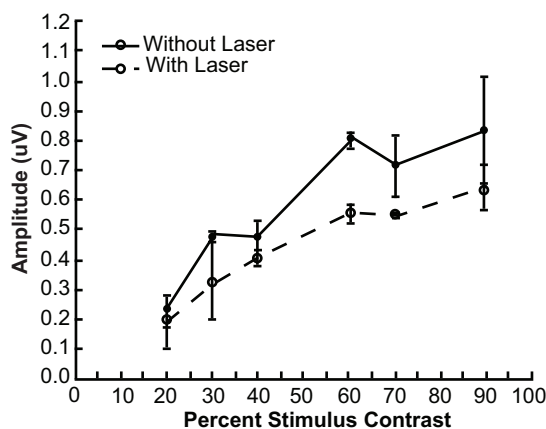


**Figure 8-23.** Effect of laser-induced lens fluorescence on visual evoked potential.

Reproduced with permission from: Zuclich JA, Glickman RD, Menendez AR. In situ measurements of lens fluorescence and its interference with visual function. *Invest Ophthalmol Vis Sci.* 1992;33:410-415.

national Commission on Illumination) chromaticity diagrams for both on-axis and  $40^\circ$  off-axis directions relative to the axis of the incident radiation. In each case, the chromaticity coordinates were plotted for three exciting wavelengths (390, 410, and 430 nm) and for each of three age categories (< 20 years, 20-45 years, and > 45 years). The results are shown in Figure 8-24 (on-axis) and Figure 8-25 (off-axis). For the on-axis measurements, color appearance reflected the relatively strong direct transmission contributions for each age group. An exception was noted only for the older lenses at the shortest exciting wavelength (390 nm), where direct transmission was minimal. By contrast, the off-axis measurements demonstrated similar fluorescent color appearances for all ages with 390-nm and 410-nm excitation, but began to reflect contributions from direct transmission of the exciting light for wavelengths as long as 430 nm. Again, the results seen in Figure 8-25 are consistent with higher transmission through the younger lenses.

Observed similarities in luminous intensities and color appearance imply that lens fluorescence and consequent glare disruption could be a comparable problem for all age categories. This was somewhat surprising since lens absorption increases and broadens with age, and so might the induced fluorescence intensity. On the other hand, the young lens is already virtually opaque (transmission < 1%) at 360 to 390 nm, and any increase in absorption beyond that level would not result in a significant incremental increase in induced fluorescence. Even at longer exciting wavelengths, where young lenses have significantly greater transmission, age-related incremental increases in induced luminance and radiance are less than a factor of 2.

Furthermore, induced lens fluorescence is generated in a cylindrical (or conical) volume as incident radiation penetrates into the lens. Therefore, even if the younger lens generates a somewhat lower fluorescent intensity, more of that fluorescence emanates from deeper within the lens. Hence, the fluorescence "source" is closer to a detector positioned behind the lens. Because emitted fluorescence must cross through intervening lens tissue before reaching the detector, and because it is more highly absorbed and scattered by older lens tissue, luminous intensity measured from the younger lens would be reduced less than that measured for the older lens. Taking this argument one step further, the in-situ scenario replaces the photometer or radiometer with the innate detector (the retina). Thus, it is inferred that the resultant visual response would be reduced less in the young lens than would otherwise be expected solely on the basis of the lower induced-fluorescent intensity.

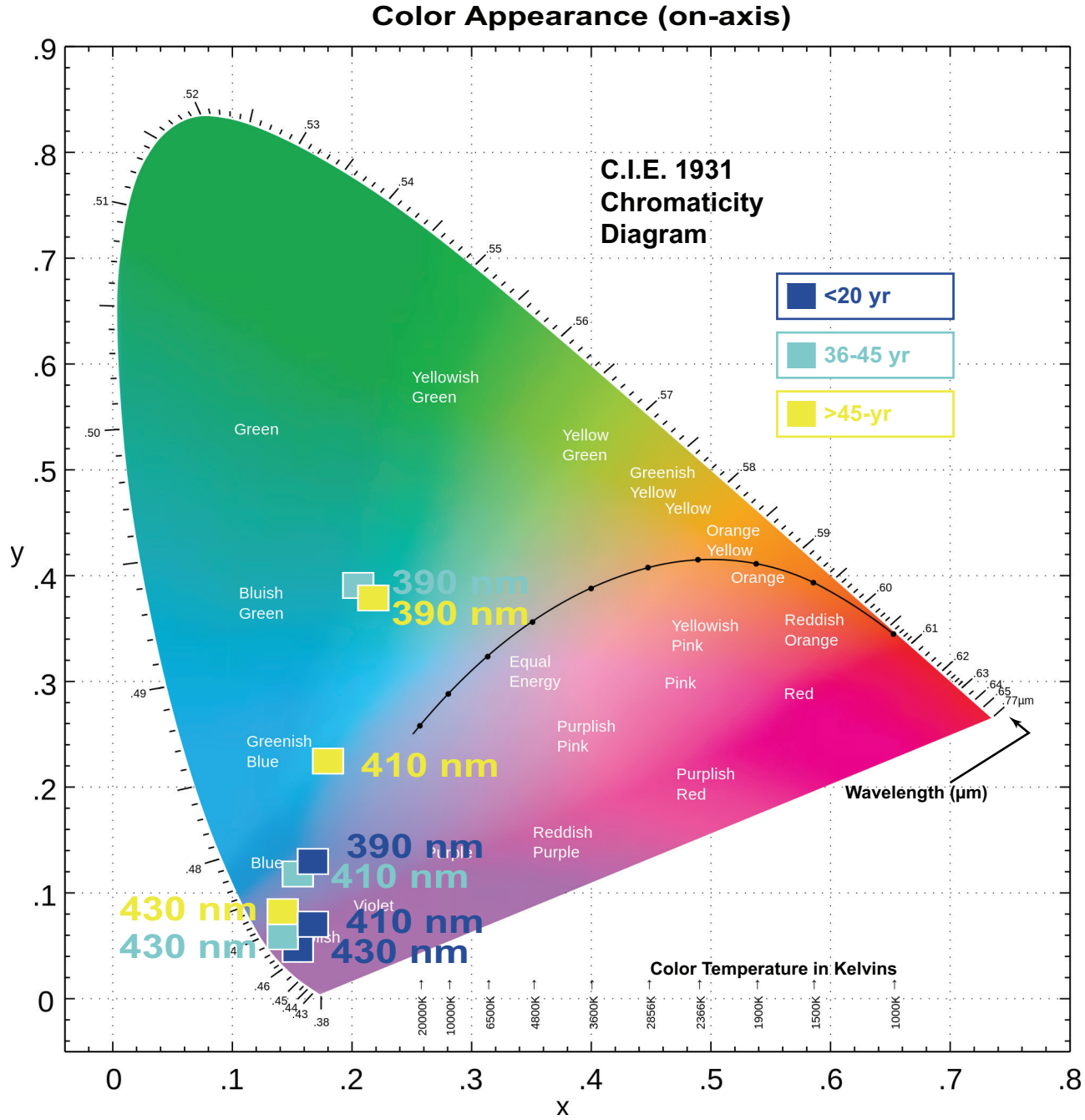


**Figure 8-24.** International Commission on Illumination (CIE) chromaticity diagram showing on-axis measurements for three exciting wavelengths and three age categories. Reproduced from: Zuclich JA, Previc FH, Novar BJ, Edsall PE. Near-UV/blue light-induced fluorescence in the human lens: potential interference with visual function. *J Biomed Optics*. 2005;10:44021-1-7. Published under Creative Commons (CC BY 4.0)-Gold Open Access (<https://creativecommons.org/licenses/by/4.0/legalcode>).

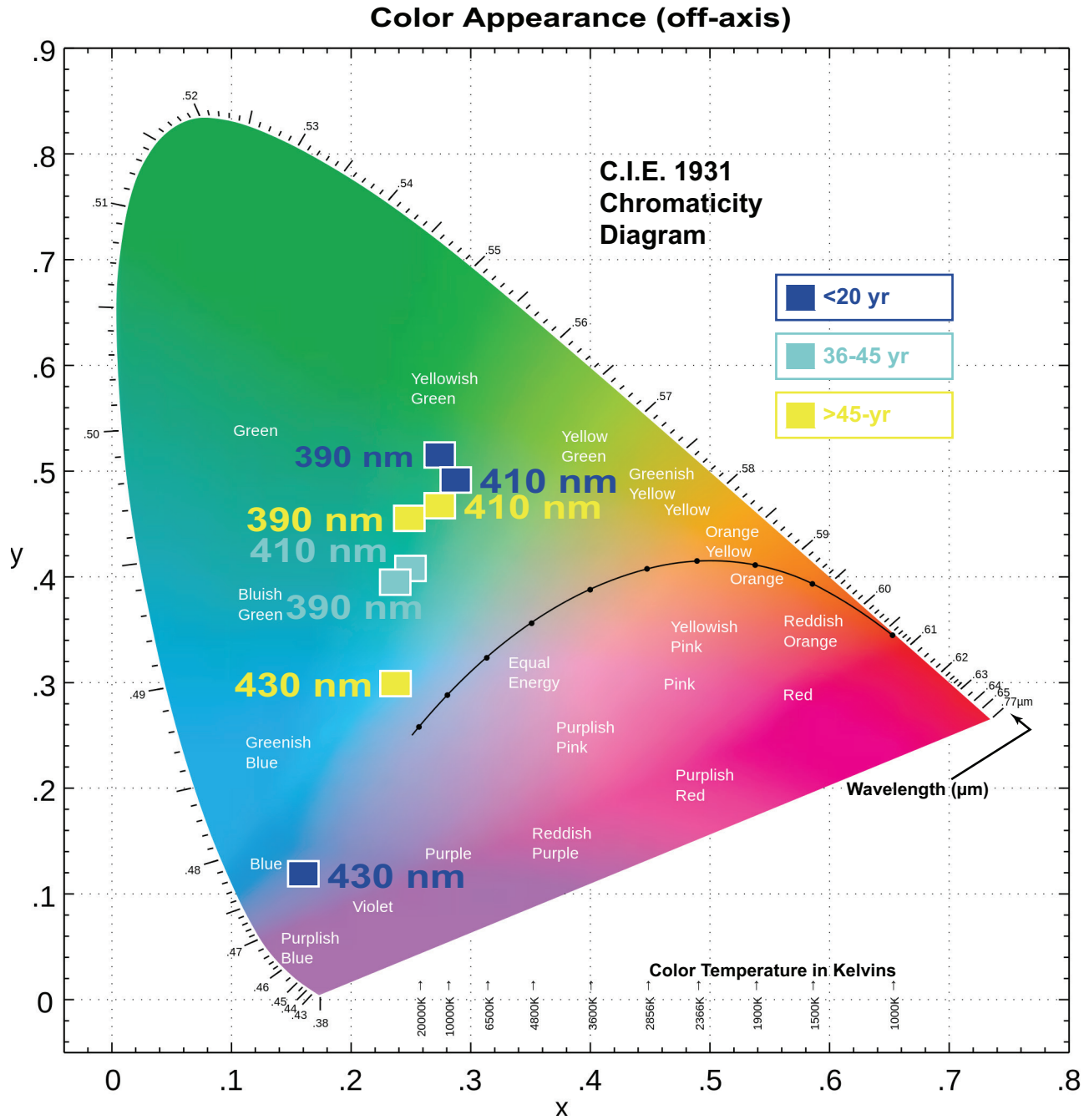


**Figure 8-25.** International Commission on Illumination (CIE) chromaticity diagram showing 40° off-axis-measurements for three exciting wavelengths and three age categories. Reproduced from: Zuclich JA, Previc FH, Novar BJ, Edsall PE. Near-UV/blue light-induced fluorescence in the human lens: potential interference with visual function. *J Biomed Optics*. 2005;10:44021-1-7. Published under Creative Commons (CC BY 4.0)-Gold Open Access (<https://creativecommons.org/licenses/by/4.0/legalcode>).

## SUMMARY

Corneal, lenticular, and retinal damage effects resulting from UV laser radiation have been described. Ranges of exposure parameters for which each of the ocular tissues is the primary target site have been identified, and in each case, the resultant UV-induced ocular pathology has been discussed. The ranges of exposure parameters suggested as capable of inducing acute effects are, necessarily, only rough guidelines because many factors individually and collectively influence the relative sensitivity of exposed ocular tissues.

Long-term (lifetime) cumulative exposures to ambient UV radiation also contribute to chronic ocular

conditions such as cataracts and macular degeneration. Exposure to low-level (subacute) doses from UV lasers or non-coherent UV sources, even if they result in no apparent short-term deleterious ocular effects, may contribute to the long-term UV cumulative "load" and thereby exacerbate the chronic consequences of UV exposure. Therefore, it falls to promulgators of laser safety standards to judiciously review evidence for the myriad reported acute and chronic consequences of UV exposures and adopt an appropriately conservative posture toward safety considerations for UV laser sources.

## REFERENCES

1. Zuclich JA. Ultraviolet laser radiation injury to the ocular tissues. In: Court LA, Duchene A, Courant D, eds. *Proceedings of the First International Symposium of Laser Biological Effects and Exposure Limits*. Cedex, France: Commissariat a l'Energie Atomique; 1988: 256-275.
2. Zuclich JA. Ultraviolet-induced photochemical damage in ocular tissues. *Health Phys.* 1989;56:671-682.
3. Boettner EA, Dankovic D. *Ocular Absorption of Laser Radiation for Calculating Personnel Hazards. University of Michigan Final Report, Contract F41609-74-C-0008*. Brooks Air Force Base, TX; US Air Force School of Aerospace Medicine; 1974.
4. Zuclich JA, Connolly JS. Ocular damage induced by near-ultraviolet laser radiation. *Invest Ophthalmol.* 1976;15:760-764.
5. Pitts DG, Tredici TJ. The effects of ultraviolet on the eye. *Am Ind Hyg Assoc J.* 1971;32:235-246.
6. Zuclich JA. Ultraviolet induced damage in the primate cornea and retina. *Curr Eye Res.* 1984;3:27-34.
7. Breschke W, Friedenwald JS, Moses SG. Effects of UV irradiation on the corneal epithelium. *J Cell Comp Physiol.* 1945;26:147-164.
8. Friedenwald JS, Breschke W, Crowell J, Hollender A. Effects of ultraviolet irradiation on the corneal epithelium II: Exposure to monochromatic radiation. *J Cell Comp Physiol.* 1948;32:161-173.
9. Kurtin WE, Zuclich JA. Action spectrum of oxygen-dependent near-ultraviolet induced corneal damage. *Photochem Photobiol.* 1978;27:329-333.
10. Mackay D, Eisenstark A, Webb RB, Brown MS. Action spectrum for lethality in recombinationless strains of salmonella typhimurium and escherichia coli. *Photochem Photobiol.* 1976;24:337-343.
11. Pitts DG. A comparative study of the effects of ultraviolet radiation on the eye. *Am J Optom Arch Am Acad Optom.* 1970;50:535-546.
12. Steiner RF, Weinryb I, eds. *Excited States of Proteins and Nucleic Acids*. New York, NY: Plenum Press; 1971.
13. Zuclich JA, Blankenstein MF. Ocular effects of ultraviolet and infrared laser radiation. In: *Effects of Laser Radiation on the Eye, Vol II*. Brooks Air Force Base, TX: US Air Force School of Aerospace Medicine; 1984. Technical Report SAM-TR-84-10.
14. Zuclich JA, Blankenstein MF. Corneal threshold for the ArF excimer laser. In: *Effects of Laser Radiation on the Eye, Vol IV*. Brooks Air Force Base, TX: US Air Force School of Aerospace Medicine; 1985. Technical Report SAM-TR-85-13.

15. Taboada J, Mikesell GW, Reed RD. Response of the corneal epithelium to KrF excimer laser pulses. *Health Phys.* 1981;40:677–683.
16. Stern D, Schoenline RW, Puliafito CA, Dobi ET, Bimgruber R, Fujimoto JG. Corneal ablation by nanosecond, picosecond, and femtosecond lasers at 532 nm and 625 nm. *Arch Ophthalmol.* 1989;107:587–592.
17. Srinivasan R. Ablation of polymers and biological tissue by ultraviolet lasers. *Science.* 1986;234:559–565.
18. Trokel SL, Srinivasan R, Braren, B. Excimer laser surgery of the cornea. *Am J Ophthalmol.* 1983;96:710–715.
19. Krueger RR, Trokel SL, Schubert HD. Interaction of ultraviolet laser light with the cornea. *Invest Ophthalmol Vis Sci.* 1985;26:1455–1464.
20. Zuclich JA. Ultraviolet laser effects on the cornea. *Proc SPIE.* 1990;1207:48–58.
21. American National Standards Institute. *American National Standard for Safe Use of Lasers.* Orlando, FL: Laser Institute of America; 2000.
22. Zuclich JA. Cumulative effects of near-UV induced corneal damage. *Health Phys.* 1980;38:833–838.
23. Griess GA, Blankenstein MF. Additivity and repair of actinic retinal lesions. *Invest Ophthalmol Vis Sci.* 1981;20:803–807.
24. Cooper GF, Robson JG. The yellow colour of the lens of man and other primates. *J Physiol.* 1969;203:411–417.
25. Waxler M, Hitchens VM. *Optical Radiation and Visual Health.* Boca Raton, FL: CRC Press; 1986.
26. Pitts DG. A comparative study of the effects of ultraviolet radiation on the eye. *Am J Optom Physiol Optics.* 1978;50:19–35.
27. Luttrull JK, Hallisey J. Laser pointer-induced macular injury. *Am J Ophthalmol.* 1999;127:95–96.
28. Sell CH, Bryan JS. Maculopathy from handheld diode laser pointer. *Arch Ophthalmol.* 1999;117:1557–1558.
29. Sethi CS, Grey RH, Hart CD. Laser pointers revisited: a survey of 14 patients attending casualty at the Bristol Eye Hospital. *Br J Ophthalmol.* 1999;83:1164–1167.
30. Zuclich JA, Stolarski DJ. Retinal damage induced by red diode laser. *Health Phys.* 2001;81:8–14.
31. Zuclich JA, Glickman RD, Menendez AR. In situ measurements of lens fluorescence and its interference with visual function. *Invest Ophthalmol Vis Sci.* 1992;33:410–415.
32. Zuclich JA, Shimada T, Loree TR, Bigio I, Strobl K, Nie S. Rapid non-invasive optical characterization of the human lens. *Lasers Life Sci.* 1994;6:39–53.
33. Zuclich JA. In vivo measurements of optical properties of the human lens. *Proc SPIE.* 1994;2134B:99–112.
34. Zuclich JA, Previc FH, Novar BJ, Edsall PE. Near-UV/blue light-induced fluorescence in the human lens: potential interference with visual function. *J Biomed Optics.* 2005;10:44021-1-7.
35. Zuclich JA, Taboada J. Ocular hazard for UV laser exhibiting self-mode locking. *Appl Optics.* 1978;17:1482–1484.
36. Ham WT, Mueller HA, Ruffolo JJ, Guerry D, Guerry RK. Action spectrum for retinal injury from near-ultraviolet radiation in the aphakic monkey. *Am J Ophthalmol.* 1982;93:299–306.
37. Schmidt RE, Zuclich JA. Retinal lesions due to ultraviolet laser exposure. *Invest Ophthalmol Vis Sci.* 1980;19:1166–1175.
38. Boettner EA. *Spectral Transmission of the Eye. University of Michigan Final Report Air Force Contract F41(609)-2966.* Brooks Air Force Base, TX: US Air Force School of Aerospace Medicine; 1967.

39. International Electrotechnical Commission. *Safety of Laser Products—Part 1: Equipment Classification, Requirements, and User's Guide*. Geneva, Switzerland: IEC; 2001.
40. Vos JJ. Disability glare—a state of the art report. *CIE J*. 1984;3:39–52.